

Surface structure analysis of thin dewetted polymer blend films

Peter Müller-Buschbaum^{1,*}, Jochen S. Gutmann², Manfred Stamm^{2,§}, Robert Cubitt³

1) TU München, Physik-Dep. LS E13, James-Franck-Str.1, 85747 Garching (Germany)

2) Max-Planck-Institut für Polymerforschung, Ackermannweg 10, 55128 Mainz (Germany)

3) ILL, Avenue des Martyrs, BP 156, 38042 Grenoble (France)

§) present address: Institut für Polymerforschung Dresden e.V., Hohe Straße 6, 01069 Dresden, Germany, stamm@ipfdd.de

SUMMARY: The surface structure of thin polymer blend films of deuterated polystyrene (dPS) and polyparamethylstyrene (PpMS) after annealing above the glass transition temperature was investigated. With scanning force microscopy (SFM) the surface topography originated by a dewetting process is detected. The sample surface is covered with small droplets consisting of several polymer molecules. Utilizing grazing incidence small angle neutron scattering (GISANS) the topographical information as well as the in-plane composition is probed. For thin confined blend films a substructure of the droplets resulting from an additional phase separation process at different length scales is detected.

Introduction

Thin polymer films are used in many applications which require special physical or chemical properties. Instead of homopolymer films in practice polymer blend films are applied. They offer a larger variety of achievable properties including the possibility of creating surface structures¹⁻⁵⁾. With spin-coating thin homogeneous polymer films may be prepared also on non-wetting surfaces. These films are metastable and small perturbations lead to a dewetting of the homogeneous film into a drop structure. The diameter of these drops depends on the original film thickness of the metastable homogeneous film^{6,7)}. In polymer blend films additionally to a dewetting process phase separation of the blend is possible. This leads to a dedicated interplay between dewetting and phase separation, which is controlled by the interactions and the compatibility of the blend components. Consequently the resulting structures are more complex including the possibility of substructures resulting from the blend. While scanning force microscopy pictures the surface topography with high resolution it yields no information about the chemical composition of the examined thin films. In case of blend components which are markedly different in their chemical composition other techniques like stiffness and friction measurements⁸⁾ or selective dissolution⁹⁾ have to be used.

For blend systems which are less immiscible like deuterated polystyrene (dPS) and polyparamethylstyrene (PpMS) these techniques deliver not enough contrast. Recently grazing incidence small angle neutron scattering (GISANS) becomes accessible for thin polymer films¹⁰⁾. Like grazing incidence small angle x-ray scattering (GISAXS) this technique offers the opportunity to determine most prominent surface in-plane structures¹¹⁻¹⁴⁾. In addition due to the reversed contrast between x-rays and neutrons a chemical composition sensitivity is achieved. In the following article we picture this by the comparison between a dewetted dPS homopolymer sample and a dPS:PpMS blend sample.

Sample preparation

On top of native oxide covered Si(100) surfaces (MEMC Electronic Materials Inc., Spartanburg) thin polymer films were prepared by spin-coating (1950rpm for 30s) a toluene solution. Prior to spin coating the silicon substrates were cleaned in a bath of 80% H₂SO₄ (100 ml), H₂O₂ (35 ml) and deionized water (15 ml) for 15 minutes at 80°C, rinsed several times in deionized water and dried with compressed nitrogen. Immediately before coating the dry substrates were flushed with fresh toluene. Deuterated polystyrene (dPS) with a molecular weight $M_w=157$ kg/mol ($M_w/M_N=1.09$, $R_g=10.6$ nm) as well as polyparamethylstyrene (PpMS) with a molecular weight $M_w=157$ kg/mol ($M_w/M_N=1.06$, $R_g=10.0$ nm) are used in an asymmetric blend composition of PpMS:dPS=60:40. From the polymer-polymer interaction parameter^{15,16)} $\chi=A+B/T$ with $A=-0.011\pm0.002$ and $B=6.8\pm1$ K we obtain $N\chi=6.6$ which pictures that the investigated blend system is only weakly incompatible. The bulk system shows a lower miscibility gap. We prepared extremely thin films by using a toluene solution with a low polymer concentration. With x-ray reflectivity the film thickness of the samples was measured right after preparation. The determined value of 3.2 ± 0.2 nm (error bar includes the deviation in the film thickness between different samples) is only 1/3 of the radius of gyration of the unperturbed molecule. Thus the polymer molecules are strongly confined. The measured rms-surface roughness of $\sigma=0.3\pm0.1$ nm agrees well with the observation of smooth and featureless surfaces in scanning force microscopy (SFM) measurements.

The samples were examined as prepared. Next they were annealed under vacuum for 8 hours at 161°C which is well above the glass transition temperature, quenched down to room temperature and examined again. In addition to the thin blend film samples homopolymer samples of dPS were prepared for comparison.

Scanning force microscopy (SFM) measurements

The real space surface topography of the as prepared as well as of the annealed samples was investigated with a PARK Autoprobe CP atomic-force microscope in air at room temperature. Several images were measured for each sample. All measurements were performed in non-contact mode in order to minimize the tip-induced sample degradation. Right after preparation with SFM no surface topography is detectable (figure 1a) which is in good agreement with the small surface roughness as determined with x-ray reflectivity. After annealing above the glass transition temperature the sample dewetted and a surface structure consisting of non-monodisperse, irregular shaped droplets results (figure 1b).

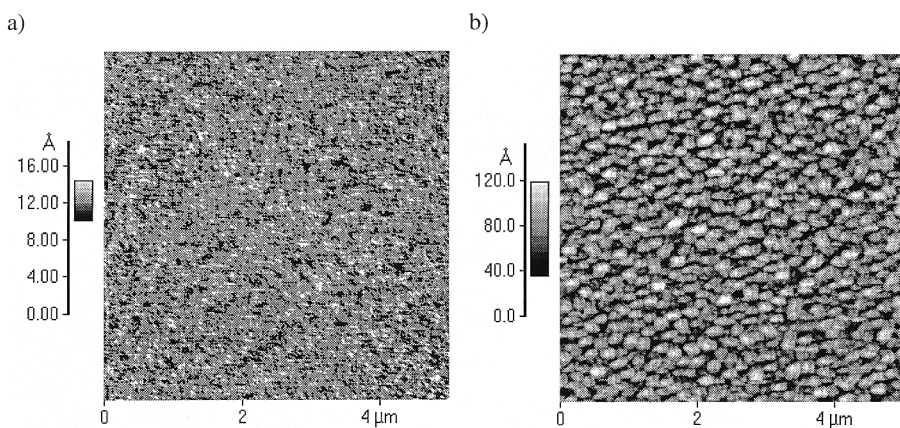


Fig. 1: Surface topography of the as prepared (a) and of the annealed (b) polymer blend film as determined with SFM. The used gray scales are different for both pictures to emphasize the detected structures.

Measurements were performed at different scan ranges between $1\mu\text{m} \times 1\mu\text{m}$ and $40\mu\text{m} \times 40\mu\text{m}$. From the surface data of each sample and scan range the two dimensional power spectral density function is calculated and radially averaged. Combining the data of different scan ranges, with respect to the individual scan size, yields a master curve¹⁷⁾ and thus enlarges the range covered by one individual power spectral density function. The resulting master curve is comparable with the scattering data (see figure 3). The one from the dewetted sample shows a well defined peak which corresponds to the mean distance between the droplets. Due to the missing monodispersity of the droplets we observe no further marked feature in the master curve.

Grazing incidence small angle neutron scattering (GISANS)

The GISANS experiments were performed at the D22 beamline at the ILL (Grenoble) at a wavelength of 0.7 nm (wavelength selector; $\Delta\lambda/\lambda = 10\%$). Thus we operate the instrument at the highest available neutron flux. Details concerning the beamline are reported elsewhere¹⁸⁾. We applied a reflection geometry with a vertically mounted sample instead of the commonly used transmission geometry (see figure 2a). The incident angle is denoted with α_i , the exit angle with α_f and the out-of plane angle with ψ . The beam divergence in and out of the plane of reflection was limited by two entrance cross slits. With a sample-detector distance of 17.66 m we achieve a resolution better than $3.81 \cdot 10^{-3} \text{ nm}^{-1}$ which enables the detection of in-plane length scales ξ up to $1.7 \text{ }\mu\text{m}$. The non-specular as well as the specular intensity was recorded with a two-dimensional detector consisting of a 128×128 pixel array.

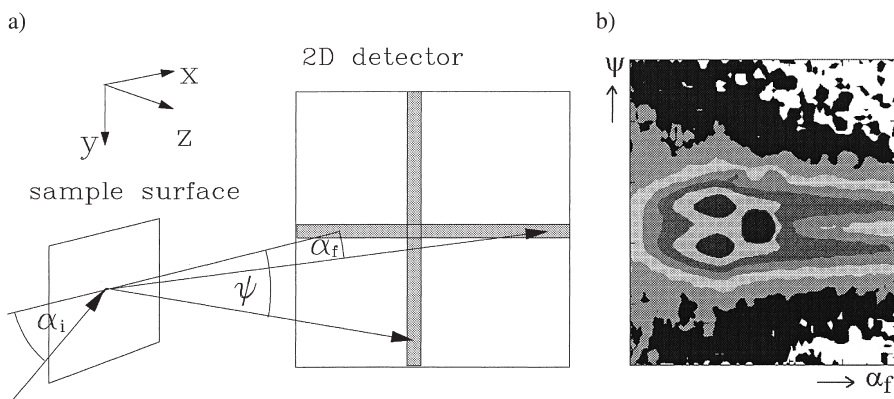


Fig. 2: (a) Schematic drawing of the experimental set-up used for the GISANS experiment and (b) example the two dimensional intensity distribution detected from the dewetted blend sample.

At $\alpha_f = \alpha_i$ the specularly reflected intensity is observed and at $\alpha_f = \alpha_c$ (critical angle) an additional peak, called Yoneda peak is measured. This dynamic feature results from the maximum of the transmission function. For isotropic samples the diffusely scattered intensity as a function of ψ is symmetric with respect to the plane of incidence ($\psi=0$). Thus it is sufficient to evaluate one half of the 2D intensity. If the sample surface is taken as the xy -plane (see figure 2a) the $\alpha_f\psi$ -intensity distribution corresponds mainly to a q_zq_y -mapping. Slices at $\psi=\text{const}$ are containing information perpendicular to the sample surface and slices at

$\alpha_f = \text{const}$ yield the in-plane information. Because the Fresnel transmission functions act in the GISANS geometry only as overall scaling factors the scattered intensity is dominated by the power spectral density function of an effective surface. Thus it is directly comparable to the master curve generated from the SFM data. Figure 3 shows the data from the dewetted blend sample in comparison to the data from the dewetted homopolymer sample and the corresponding master curve calculated from the SFM data.

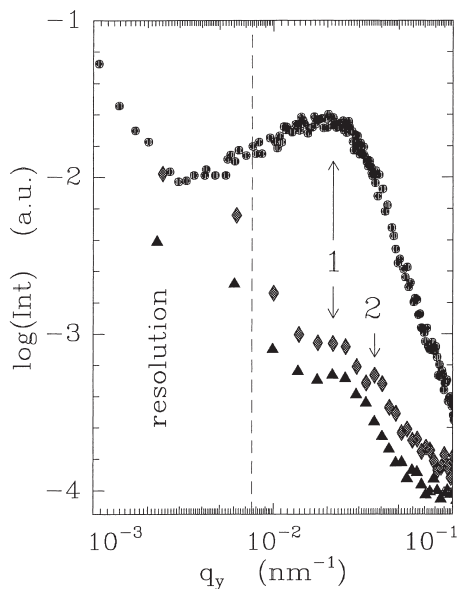


Fig. 3: Double logarithmic plot of the scattered intensity from the dewetted blend (rhomb) and from the dewetted homopolymer (triangle) sample as a function of the in-plane wave vector q_y . For a comparison the master curve (dots) is shown. The resolution limit is represented by the dashed line. The most prominent in-plane length scale leads to a peak in the intensity at the position marked with "1". In the data of the blend sample an additional peak is observable (marked "2").

The three data sets exhibit a peak at the position marked with "1". It corresponds to the most prominent in-plane length scale of $\xi_1 = 293 \pm 5$ nm and pictures the distance between individual droplets. Because it is visible in the master curve from the SFM data as well as in the scattering data it is a pure topological information. The data of the blend sample show a second peak resulting from a smaller length scale of $\xi_2 = 171 \pm 2$ nm (marked "2") which appears to have a smaller FWHM due to the logarithmic x-axis. It should be noted that, in the master curve from the SFM data (dots) this peak at ξ_2 is invisible, whereas the peak at ξ_1 is even more pronounced. Thus ξ_2 corresponds to a composition length scale and is due to an internal structure of the droplets. Although the dewetting itself is not driven by the polymer incompatibility in the investigated confined blend films of PpMS:dPS there is some trend to a phase separation. As compared to the radius of gyration of the unperturbed molecules of $R_g = 10$ nm the observed structures are large and thus consist of numerous molecules.

Conclusion

The surface topography of the confined, annealed polymer films exhibits one most prominent in plane length scale which corresponds to the mean distance of the droplets originated by the dewetting. This in-plane length is detected with SFM and with GISANS and therefore can be regarded as representative for the whole sample. In case of the polymer blend sample a further substructure is detected with GISANS. It results from composition inhomogenities due to a phase separation process. Thus GISANS combines the typical advantages of neutron experiments with advanced scattering techniques commonly used with x-rays. It is well suited to probe the roughness spectrum from a molecular to mesoscopic in-plane length scale and it provides information about the internal composition of the examined samples.

Acknowledgments

This work was supported by the DFG Schwerpunktprogramm "Benetzung und Strukturbildung an Grenzflächen" (Sta 324/8-1) and J.S.G. acknowledges support by the GKSS project V6.1.01.G.01-HS3.

References

1. G. Krausch, *Mater. Sci. Eng.* **R14**, 1 (1995)
2. S. Affrossman, G. Henn, S. A. O'Neill, R. A. Pethrick, M. Stamm, *Macromolecules* **29**, 5010 (1996)
3. L. Sung, A. Karim, J. F. Douglas, C. C. Han, *Phys. Rev. Lett.* **76**, 4368 (1996)
4. K. D. Jandt, J. Heier, F. S. Bates, E. J. Kramer, *Langmuir* **12**, 3716 (1996)
5. E. Kumacheva, L. Li, M. A. Winnik, D. M. Shinozaki, P. C. Cheng, *Langmuir* **13**, 2483 (1997)
6. F. Brochard-Wyart, C. Redon, C. Sykes, *C.R.Acad.Sci.Ser.2* **19**, 314 (1992)
7. G. Reiter, *Phys.Rev.Lett* **68**, 75 (1992)
8. G. Krausch, M. Hipp, M. Böltau, J. Mlynek, *Macromolecules* **28**, 260 (1995)
9. S. Walheim, M. Böltau, J. Mlynek, G. Krausch, U. Steiner, *Macromolecules* **30**, 4995 (1997)
10. P. Müller-Buschbaum, J. S. Gutmann, M. Stamm, *PCCP*, at press
11. T. Salditt, T. H. Metzger, J. Peisl, B. Reinker, M. Moske, K. Samwer, *Europhys. Lett* **32**, 331 (1995)
12. P. Müller-Buschbaum, P. Vanhoorne, V. Scheumann, M. Stamm, *Europhys. Lett.* **40**, 655 (1997)
13. P. Müller-Buschbaum, M. Casagrande, J. Gutmann, T. Kuhlmann, M. Stamm, S. Cunis, G. von Krosigk, U. Lode, R. Gehrke, *Europhys. Lett.* **42**, 517 (1998)
14. P. Müller-Buschbaum, M. Stamm, *Physica B* **248**, 229 (1998)
15. W. G. Jung, E. W. Fischer, *Makromol. Chem., Macromol. Symp.* **16**, 281 (1988)
16. R. Schnell, M. Stamm, *Physica B* **234-236**, 247 (1997)
17. J. S. Gutmann, P. Müller-Buschbaum, M. Stamm, *Faraday Discuss.* **112**, at press
18. H. G. Büttner, E. Lelievre-Berna, F. Pinet, *Guide to Neutron Research Facility at the ILL*, 32 (1997)